


Atomic Manipulation on a Highly Corrugated Topological Insulator

Emma Grasser¹,[†] Adrian Weindl¹,^{†,*} Alfred J. Weymouth¹, and Franz J. Giessibl¹

Institute of Experimental and Applied Physics, University of Regensburg, Regensburg D-93053, Germany

 (Received 5 June 2024; revised 14 October 2024; accepted 20 February 2025; published 20 March 2025)

We report a mechanism of lateral manipulation of single Fe adatoms on the surface of the topological insulator Bi_2Se_3 with atomic force microscopy. The Fe atoms are embedded within the sparsely packed surface layer, rendering them inaccessible to classical manipulation methods. Nevertheless, we find a manipulation mechanism in which the Fe atom is plucked from its adsorption site and can be pulled along the surface. We demonstrate the controllability of this pluck-pull manipulation by the construction of a small nanostructure.

DOI: [10.1103/PhysRevLett.134.116201](https://doi.org/10.1103/PhysRevLett.134.116201)

In 1990, Eigler and Schweizer manipulated single Xe atoms on a Ni(100) surface with a scanning tunneling microscope [1]. This was the birth of single-atom manipulation that enabled the creation of artificial nanostructures [2–6]. Adsorbates are often manipulated with the tip of a scanning probe microscope via lateral and vertical manipulation methods [7–11]. In lateral manipulation, classically divided into pushing, pulling, and sliding motions [8], the tip directly interacts with the adsorbate, either repulsively (pushing) or attractively (pulling). Sliding involves stronger vertical attraction with the tip and the adsorbate continuously follows the tip motion, in contrast to discrete jumps to adjacent adsorption sites as observed in manipulation by pulling. In all cases, interaction with the surface is dominant, so that when the tip retracts, the adsorbate remains on the surface. This is in contrast to vertical manipulation, where the adsorbate moves to the tip and is stable there until it is controllably deposited back onto the surface. Vertical manipulation can be used to access partially or fully embedded adsorbates [12,13]. However, lateral manipulation of embedded atoms remains challenging. For example, a Sn atom on Ge(111) can be exchanged for a Ge atom at a different lateral position, but this requires a system where Sn and Ge sit in equivalent sites and can exchange positions repeatedly [14].

A system with strong practical relevance where these classical manipulation methods do not work is Fe atoms on a Bi_2Se_3 surface. Bi_2Se_3 is a topological insulator and as such has a bulk band gap and metallic surface states that exhibit a linear dispersion [15,16]. These surface states are spin polarized and time-reversal symmetric, resulting in a strong suppression of backscattering. Fe is proposed to be a magnetic scatterer [17] and as such expected to break time-reversal symmetry. Magnetic

impurities can allow for various exotic phenomena to arise in topological insulators [18–20]. These impurities must have a large magnetic moment and specific magnetic anisotropy, properties that depend strongly on the exact coordination and adsorption site [21,22]. The ability to manipulate magnetic atoms on topological insulator surfaces opens exciting new research avenues. In previous work, it was proposed that Fe adatoms adsorb on Bi_2Se_3 in hollow sites in the plane (± 10 pm) of the surface atoms, as determined by a combination of scanning tunneling microscopy (STM) and density functional theory (DFT) [17]. This means the atoms do not sit on the surface but rather are embedded within it and are therefore inaccessible via standard manipulation techniques.

In this Letter, we report a mechanism of lateral manipulation, where single Fe atoms embedded into the surface of Bi_2Se_3 are plucked from their adsorption sites and subsequently trapped between tip and surface by developing a chemical bond to the tip. Using atomic force microscopy (AFM) [23] and spectroscopy, we show that the Fe follows the tip for up to several angstrom in vertical distance and that it can be laterally pulled across the surface.

Bi_2Se_3 is a layered material consisting of weakly bound quintuple layers with stacking order Se-Bi-Se-Bi-Se. Upon cleavage, the surface is terminated by such a quintuple layer and, hence, a Se layer [24]. The surface Se atoms are spaced by a lattice constant of 414 pm [25]. The radius of covalently bound Se at 107 pm [26] is rather small compared to the lattice spacing, meaning it is sparsely packed. Iron atoms were deposited on the cold (4.4 K) substrate using an electron-beam evaporator.

Figure 1(a) shows an AFM scan of two single Fe atoms adsorbed on the Bi_2Se_3 surface recorded using a CO-terminated tip [27]. Fe_A and Fe_B , appearing as starlike features, differ by 60° in orientation. They adsorb in the fcc and hcp hollow sites, but as the AFM does not provide access to the atomic configuration of subsurface layers, we cannot assign specific hollow sites to the Fe adatoms. From

*Contact author: adrian.weindl@ur.de

[†]These authors contributed equally to this work.

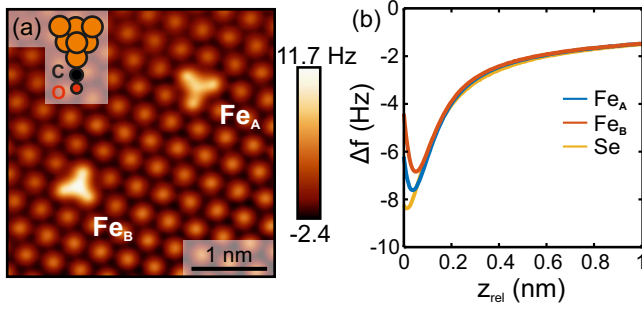


FIG. 1. Single Fe adatoms adsorbed on the Bi_2Se_3 surface measured using a CO-terminated tip. (a) Constant height AFM image of two Fe adatoms adsorbed in inequivalent hollow sites. Inset: a schematic depiction of a CO-terminated metal tip. (b) $\Delta f(z)$ spectra recorded on two Fe atoms in different hollow sites and a surface Se atom. Here, $z_{\text{rel}} = 0$ corresponds to the point of closest approach with the CO tip.

Δf versus z spectra, recorded on a Se surface atom and two Fe atoms [see Fig. 1(b)], the apparent relative adsorption heights can be extracted. This yields adsorption heights relative to the surface Se layer of 23 pm ($\pm 5\%$) for Fe_A and 38 pm ($\pm 10\%$) for Fe_B . These values are similar to those previously reported [17] and confirm that the Fe atoms embed into the surface layer. An important factor in single-atom manipulation experiments is the atomic configuration of the probe tip apex. Tips terminated by a different number or species of atoms can yield vastly differing results [28]. We attempted manipulation with CO-terminated tips, single-atom metal tips, and three-atom metal tips.

The CO tip is most favorable in terms of spatial resolution and chemical stability but it has a low lateral stiffness [29–31]. In our experiments, CO tips were unable to perform manipulation. It is likely the attraction between CO tips and Fe adatoms is too weak. We propose that the lateral forces never surpassed the threshold for manipulation and, instead, the CO molecule deflected at close tip-sample separation.

We therefore attempted manipulation using single-atom metal tips, i.e., metal tips that end in a single atom. The tip apex was confirmed with the carbon monoxide front atom identification method (see Fig. S1 in Supplemental Material [32]), as discussed in [38]. Metal tips exhibit a much larger lateral stiffness than CO tips and a greater attractive force to Fe adatoms, and we therefore expected them to perform better at manipulation. While capable of manipulating Fe atoms on Bi_2Se_3 , the single-atom metal tips often underwent structural changes shortly after approaching to the surfaces due to tip and surface being quite reactive. Therefore, while possible, manipulation with single-atom metal tips carries the constant risk of unintentionally modifying the tip, potentially rendering it unusable for further manipulation attempts.

The three-atom metal tip, which is a metal tip ending in three atoms, turned out to be the most reliable. This balance between single-atom tips that are too reactive and trimer tips that have just the right reactivity has previously been

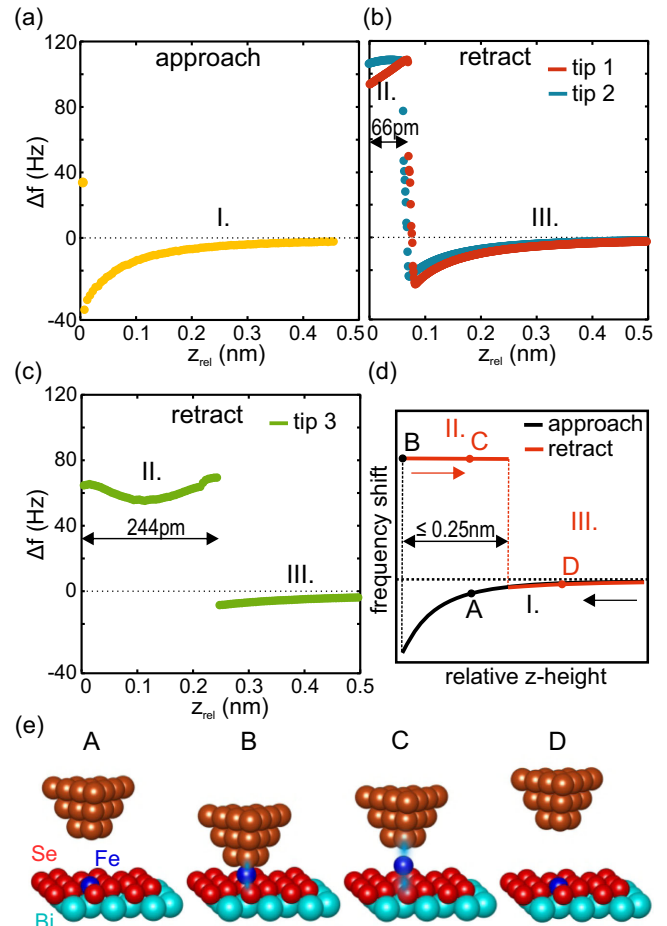


FIG. 2. $\Delta f(z)$ spectra recorded on Fe adatoms on Bi_2Se_3 . (a) Experimental approach curve (with zero bias voltage and $z_{\text{rel}} = 0$ being the manipulation height). (b),(c) Experimental retraction curves. A different tip was used for recording each of the spectra. (d) Schematic $\Delta f(z)$ curve during the approach (black) and retraction (red) of the AFM tip. A large jump in Δf signal indicates the onset of manipulation. A second jump in the opposite direction marks the end of manipulation. (e) Schematic representation of the tip-sample system at relevant points during approach and retraction of the AFM tip.

observed in imaging graphene [39]. It was also found that two- or three-atom In tips are required for the manipulation of In adatoms on $\text{InAs}(111)$ [13]. As the three-atom metal tip is able to manipulate Fe and operate on Bi_2Se_3 for prolonged durations without frequent structural changes, we consider it to be optimal for manipulating Fe. While tip changes did occasionally occur, they were usually minor and did not prevent further manipulation. All of the following data were recorded using three-atom metal tips.

We first present the interaction of the Fe adsorbate with the tip as a function of the vertical distance. While individually measured spectra [Figs. 2(a)–2(c)] are slightly different, the overall shape of the tip-sample interaction is the same and shown schematically in Fig. 2(d). When the tip-sample distance is reduced (I), the Δf value decreases

until a sudden increase in Δf occurs, reaching values of 40 Hz and higher [Fig. 2(a)]. Δf values as large as these are often associated with a structural change of the system [40,41]. During tip retraction, the Δf signal varies slightly, but remains positive (II). Only at a certain tip-sample distance, after up to several hundreds of picometers away, the Δf signal drops significantly, returning to negative values [Figs. 2(b) and 2(c)]. From this point on, the spectra follow the characteristic shape of Δf versus z curves on this surface (III).

Our interpretation is shown conceptually in Fig. 2(e). Initially, the Fe adatom is embedded in the surface, with the three closest Se atoms relaxing outward. Once the tip is sufficiently close, the Fe atom is plucked from its adsorption site, at which point it is bound to both tip and surface. This state is stable even when the vertical position of the tip is varied by up to several hundreds of picometers. Finally, the sharp drop in the Δf retraction curve indicates the end of manipulation, where the Fe falls back to the sample. In a few cases ($\approx 18\%$), it vanished, presumably jumping to the tip.

Positive Δf values are usually associated with repulsion. However, the frequency shift Δf is rather a measure of the weight-averaged force gradient over one oscillation cycle along the z direction, than the force itself [42], i.e., positive Δf is equivalent to positive curvature in the interaction potential. Below, in the discussion of Fig. 3, we will argue that the force acting between tip and Fe atom is attractive. This means that the Fe atom is very close to the tip throughout the whole manipulation process, as positive Δf and attractive forces only coexist near the minimum of interatomic potentials (see Fig. S2 in Supplemental Material [32]).

We propose that the mechanism of the plucking of the Fe atom is similar to the mechanism of wire formation [43], which has been reported for various surfaces and exhibits a characteristic distance-dependent conductance signal very similar to what we observe for Fe on Bi_2Se_3 (see Fig. S6 in Supplemental Material [32]) [43–47]. There is further evidence for wire formation in instances where tip retraction does not result in the single Fe atom returning to the surface: We have observed infrequent cases (less than 5% of cases) with even larger z ranges (exceeding 400 pm) of positive Δf with very pronounced variations in the spectrum and resulted in clusters of tip atoms being present on the sample surface afterward (see Fig. S3 in Supplemental Material [32]).

As described above, we observe large z ranges of up to several angstrom for which the Fe adatom remains slightly lifted in between the tip and surface. In this range (region II in Fig. 2) the Fe can be moved laterally in arbitrary directions along the surface of Bi_2Se_3 . This controlled lateral manipulation of the Fe atoms allows for the construction of atomic-scale nanostructures. The ability to controllably move adsorbates that strongly relax within the

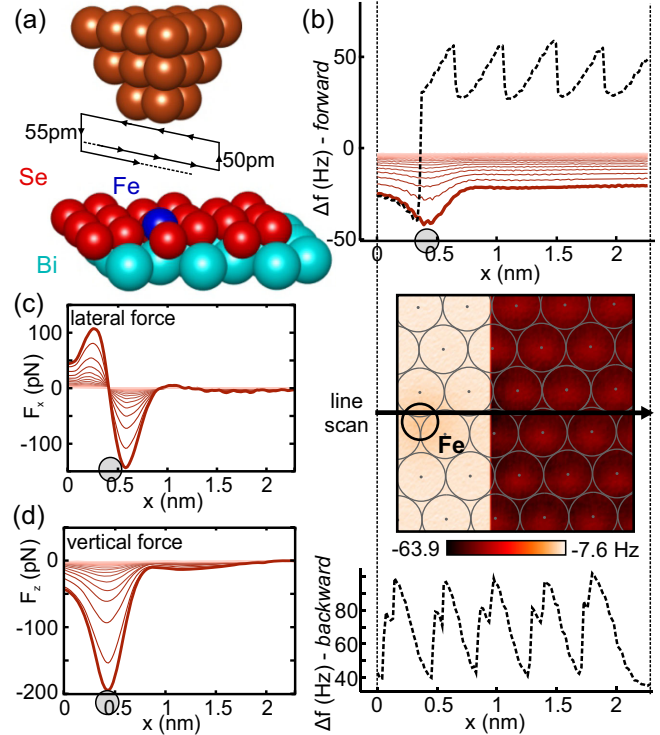


FIG. 3. Lateral manipulation of Fe on Bi_2Se_3 . (a) Schematic of the scanning process for recording of lateral and vertical forces. The three-atom tip is scanned repeatedly across the Fe adatom and approached to the surface by 5 pm after each pass. (b) Constant height AFM image (middle) of Fe on the Se surface before manipulation (the tip-sample distance in the right part is 200 pm smaller than in the left part). The frequency shift as a function of the lateral distance was recorded along the line marked by the black arrow in the AFM image. The Δf profiles (top) during the approach, getting closer to the surface by 25 pm for each line (the intermediate steps at 5 pm intervals are not shown here for the sake of clarity). The black dashed line shows the curve during manipulation itself and the gray circle the position of the Fe atom. The backward scan of the last Δf profile (bottom) was measured with 50 pm larger tip-sample distance. (c) Lateral and (d) vertical force during the approach calculated from the Δf line scans in (b).

top surface layer provides access to a large number of systems where manipulation was previously considered to not be feasible.

The formation of a bond between the adsorbate and tip to allow for lateral manipulation, as we propose is the case here, has been observed previously for mobile adsorbates on $\text{Si}(111)-7 \times 7$ [48]. There, the adsorbates can be trapped underneath the tip of a STM and, upon retraction of the tip, they remain trapped for a z range of around 1 Å before resuming their diffusive movement. DFT calculations revealed that a bond between the tip and the respective adatom is responsible for the trapping and crucial to the manipulation of the adatom [49]. This is in contrast to bond formation in atomic-scale contacts where no significant

relaxation of tip atoms and/or adsorbates is observed. In these cases, the $\Delta f(z)$ and force spectra do not exhibit hysteretic behavior and are smooth [50,51].

When the Fe is plucked from its adsorption site, it can be pulled across the Bi_2Se_3 surface. To evaluate the lateral and vertical forces during manipulation, we acquired line scans across the adsorbate in the desired manipulation direction, starting from a height where there is no contrast in the Δf signal. For each subsequent forward scan, the tip-sample distance was reduced by 5 pm. During the backward scans, the tip was retracted by 50 pm [see Fig. 3(a)]. This process was repeated until the adsorbate had been manipulated.

Figure 3(b) shows an AFM image of an Fe atom together with Δf profiles recorded during the manipulation procedure. The AFM image was measured without feedback with the left side at a higher z value to determine the position of the Fe atom and the right side at a lower z value for atomic resolution of the Se layer. The black arrow, indicating the manipulation path, runs along the hollow sites identical to the one the Fe atom is adsorbed in. The frequency shift recorded in the forward direction shows no contrast for high tip-sample distances. At intermediate heights, the Fe appears as a shallow dip in the frequency shift and, with decreasing height, this dip becomes deeper. Going even closer, manipulation occurs, recognizable by a large jump in Δf signal to high positive values [black dotted line in the forward scans in Fig. 3(b)]. Beyond this point, the profile exhibits a regular, sawtoothlike pattern. The spacing of the minima is about 413 pm, in agreement with the lattice constant measured for the surface of Bi_2Se_3 . We therefore attribute this to the Fe atom hopping from one hollow site to the next. The backward scan [Fig. 3(b)], for which the tip is retracted by 50 pm, shows a similar behavior, though with additional weaker dips. This shows that the Fe atom can be manipulated laterally on the surface in a z range of at least 50 pm. The additional structure in the Δf profile for the backward scan may indicate that there are different transitional adsorption sites during manipulation, depending on the tip-sample distance. While here only movement in one direction is shown, it is possible to pull the Fe atoms in any direction and along arbitrary paths on the surface. However, the Fe atoms could only be deposited in one of the two hollow sites (type B). This supports the idea of the Fe atom hopping along identical hollow sites spaced by a lattice constant in Fig. 3(b).

Figure 3(c) shows the lateral force calculated from the Δf curves in Fig. 3(b). Positive values correspond to a force pointing in positive x direction, i.e., along the manipulation path. The force curves in Fig. 3(c) all show positive forces before the tip has passed the center of the Fe adatom, i.e., the tip and the Fe attract each other. After having passed the center of the adsorbate, the lateral force becomes negative, again indicating attractive interaction between tip and adatom. Hence, the force between tip and Fe adatom is always attractive. This was observed for all manipulation

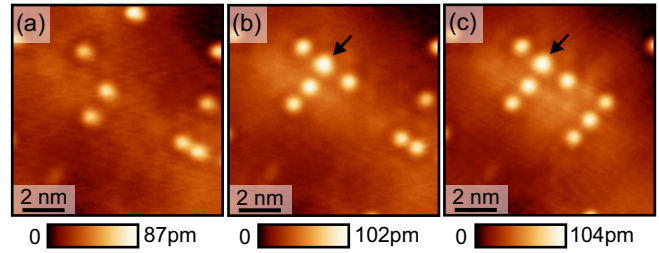


FIG. 4. STM images depicting manipulation of Fe adatoms to form the letters “TI”. (a) All Fe atoms are still at their initial position. (b) Intermediate result, where several Fe adatoms have been moved to form the letter “T.” (c) The letters TI built from Fe adatoms are complete. Note, that the atom marked with the black arrow is of unknown type.

attempts. The fact that the vertical force is negative throughout the approach [Fig. 3(d)] means that it is overall attractive. This, coupled with the fact that during manipulation the Fe atom follows the tip, regardless of scan direction and within a tip z range of several hundreds of pm, leads us to conclude that when the Fe atom is plucked from the adsorption site, it still interacts predominantly via attraction with the tip despite positive Δf values. To illustrate the controllability of this pluck-pull manipulation of Fe on Bi_2Se_3 , the letters TI were formed. Figures 4(a)–4(c) show STM images recorded before, during, and after building the letters. Note that the atom marked with the black arrow is an adsorbate of unknown type, which appeared during a manipulation attempt. Constant height AFM images reveal that all of the Fe adatoms forming the TI letters are adsorbed in equivalent sites (see Fig. S4 in Supplemental Material [32]). The adsorbate marked in Fig. 4 is not adsorbed in a hollow site and does not show the typical AFM signature of Fe adatoms on Bi_2Se_3 . We think it most likely consists of one or more atoms dropped from the tip. The overall success rate of manipulation using single- and three-atom metal tips was $\approx 40\%$.

In summary, we report a novel mechanism of lateral manipulation of single Fe adatoms on the highly corrugated surface of topological insulator Bi_2Se_3 . We found that manipulation is possible in spite of the Fe atoms being embedded in the surface. The optimal tip configuration was the three-atom metal tip, which proved to be both stable and capable of manipulating Fe atoms. Investigating the tip interaction as a function of vertical distance led us to propose that the Fe atom is plucked upon tip approach and dropped back to the surface at larger tip-sample distances of up to several hundreds of picometers away. Manipulation experiments showed purely attractive interaction, supporting the idea of a bond forming between Fe atom and tip. We demonstrated controllability of the pluck-pull manipulation and the possibility to construct nanostructures of Fe on Bi_2Se_3 . Bi_2Se_3 is part of the $\text{Bi}_{2-x}\text{Sb}_x\text{Te}_y\text{Se}_{3-y}$ family of topological insulators, all of which possess similar crystal structures. We propose that the lateral

manipulation mechanism presented here can be used to construct artificial nanostructures on these materials. This would allow not only for the observation of quantum chaos [52] and quantum mirages [53] but also the determination of the potential and magnetic scattering strengths of adsorbates, which is of interest in the design of TI-based devices [54].

Acknowledgments—We thank the Deutsche Forschungsgemeinschaft (SFB 1277, Project No. 314695032) for funding.

E. G. and A. W. contributed equally to this work. E. G. and A. W. performed the experiments and analyzed the data. E. G. wrote the initial draft and A. W. wrote the final version of the manuscript. A. J. W. assisted with data analysis and drafting of the manuscript. F. J. G. conceived the research and supervised the project.

-
- [1] D. M. Eigler and E. K. Schweizer, *Nature (London)* **344**, 524 (1990).
- [2] M. F. Crommie, C. P. Lutz, and D. M. Eigler, *Science* **262**, 218 (1993).
- [3] L. Schneider, K. T. Ton, and I. Ioannidis, *Nature (London)* **621**, 60 (2023).
- [4] E. Sierda, X. Huang, D. I. Badrtdinov, B. Kiraly, E. J. Knol, G. C. Groenenboom, M. I. Katsnelson, M. Rösner, D. Wegner, and A. A. Khajetoorians, *Science* **380**, 1048 (2023).
- [5] S. N. Kempkes, M. R. Slot, J. J. van den Broeke, P. Capicod, W. A. Benalcazar, D. Vanmaekelbergh, D. Bercioux, I. Swart, and C. Morais Smith, *Nat. Mater.* **18**, 1292 (2019).
- [6] W. Jolie, T.-C. Hung, L. Niggli, B. Verlhac, N. Hauptmann, D. Wegner, and A. A. Khajetoorians, *ACS Nano* **16**, 4876 (2022).
- [7] G. Meyer, B. Neu, and K. H. Rieder, *Appl. Phys. A* **60**, 343 (1995).
- [8] L. Bartels, G. Meyer, and K.-H. Rieder, *Phys. Rev. Lett.* **79**, 697 (1997).
- [9] M. Ternes, C. P. Lutz, C. F. Hirjibehedin, F. J. Giessibl, and A. J. Heinrich, *Science* **319**, 1066 (2008).
- [10] O. Custance, R. Perez, and S. Morita, *Nat. Nanotechnol.* **4**, 803 (2009).
- [11] Q. Zhong, A. Ihle, S. Ahles, H. A. Wegner, A. Schirmeisen, and D. Ebeling, *Nat. Chem.* **13**, 1133 (2021).
- [12] J. Yang, C. Nacci, J. Martínez-Blanco, K. Kanisawa, and S. Fölsch, *J. Phys. Condens. Matter* **24**, 354008 (2012).
- [13] R. A. M. Ligthart, C. Coinon, L. Desplanque, X. Wallart, and I. Swart, *SciPost Phys.* **16**, 096 (2024).
- [14] Y. Sugimoto, M. Abe, S. Hirayama, N. Oyabu, O. Custance, and S. Morita, *Nat. Mater.* **4**, 156 (2005).
- [15] H. Zhang, C.-X. Liu, X.-L. Qi, X. Dai, Z. Fang, and S.-C. Zhang, *Nat. Phys.* **5**, 438 (2009).
- [16] Y. Xia, D. Qian, D. Hsieh, L. Wray, A. Pal, H. Lin, A. Bansil, D. Grauer, Y. S. Hor, R. J. Cava, and M. Z. Hasan, *Nat. Phys.* **5**, 398 (2009).
- [17] J. Honolka, A. A. Khajetoorians, V. Sessi, T. O. Wehling, S. Stepanow, J.-L. Mi, B. B. Iversen, T. Schlenk, J. Wiebe, N. B. Brookes, A. I. Lichtenstein, P. Hofmann, K. Kern, and R. Wiesendanger, *Phys. Rev. Lett.* **108**, 256811 (2012).
- [18] Y. L. Chen, J.-H. Chu, J. G. Analytis, Z. K. Liu, K. Igarashi, H.-H. Kuo, X. L. Qi, S. K. Mo, R. G. Moore, D. H. Lu, M. Hashimoto, T. Sasagawa, S. C. Zhang, I. R. Fisher, Z. Hussain, and Z. X. Shen, *Science* **329**, 659 (2010).
- [19] R. Yu, W. Zhang, H.-J. Zhang, S.-C. Zhang, X. Dai, and Z. Fang, *Science* **329**, 61 (2010).
- [20] S.-Y. Xu *et al.*, *Nat. Phys.* **8**, 616 (2012).
- [21] D. West, Y. Y. Sun, S. B. Zhang, T. Zhang, X. Ma, P. Cheng, Y. Y. Zhang, X. Chen, J. F. Jia, and Q. K. Xue, *Phys. Rev. B* **85**, 081305(R) (2012).
- [22] M. Chrobak, K. Maćkosz, M. Jurczyszyn, M. Dobrzański, K. Nowak, T. Ślezak, M. Zajac, M. Sikora, M. Rams, T. Eelbo, J. Stepień, M. Waśniowska, O. Mathon, F. Yakhou-Harris, D. G. Merkel, I. Miotkowski, Z. Kakol, A. Kozłowski, M. Przybylski, and Z. Tarnawski, *New J. Phys.* **22**, 063020 (2020).
- [23] G. Binnig, C. F. Quate, and C. Gerber, *Phys. Rev. Lett.* **56**, 930 (1986).
- [24] D. D. dos Reis, L. Barreto, M. Bianchi, G. A. S. Ribeiro, E. A. Soares, W. S. o. e. Silva, V. E. de Carvalho, J. Rawle, M. Hoesch, C. Nicklin, W. P. Fernandes, J. Mi, B. B. Iversen, and P. Hofmann, *Phys. Rev. B* **88**, 041404(R) (2013).
- [25] A. Cavallin, V. Sevriuk, K. N. Fischer, S. Manna, S. Ouazi, M. Ellguth, C. Tusche, H. L. Meyerheim, D. Sander, and J. Kirschner, *Surf. Sci.* **646**, 72 (2016).
- [26] P. Pyykkö, S. Riedel, and M. Patzschke, *Chem. Eur. J.* **11**, 3511 (2005).
- [27] L. Gross, F. Mohn, N. Moll, P. Liljeroth, and G. Meyer, *Science* **325**, 1110 (2009).
- [28] D. Yesilpinar, B. Schulze, A. Timmer, Z. Hu, W. Ji, S. Amirjalayer, H. Fuchs, and H. Mönig, *Small* **17**, 2101637 (2021).
- [29] N. Moll, L. Gross, F. Mohn, A. Curioni, and G. Meyer, *New J. Phys.* **12**, 125020 (2010).
- [30] A. J. Weymouth, T. Hofmann, and F. J. Giessibl, *Science* **343**, 1120 (2014).
- [31] S. K. Hämäläinen, N. van der Heijden, J. van der Lit, S. den Hartog, P. Liljeroth, and I. Swart, *Phys. Rev. Lett.* **113**, 186102 (2014).
- [32] See Supplemental Material at <http://link.aps.org/supplemental/10.1103/PhysRevLett.134.116201> for instrumentation, additional images, and analysis, which includes Refs. [33–37].
- [33] L. Bartels, G. Meyer, and K.-H. Rieder, *Appl. Phys. Lett.* **71**, 213 (1997).
- [34] F. J. Giessibl, *Rev. Sci. Instrum.* **90**, 011101 (2019).
- [35] J. Welker and F. J. Giessibl, *Science (New York, N.Y.)* **336**, 444 (2012).
- [36] J. E. Sader and S. P. Jarvis, *Appl. Phys. Lett.* **84**, 1801 (2004).
- [37] F. Huber and F. J. Giessibl, *J. Appl. Phys.* **127**, 184301 (2020).
- [38] O. Gretz, A. J. Weymouth, and F. J. Giessibl, *Phys. Rev. Res.* **2**, 033094 (2020).
- [39] T. Hofmann, X. Ren, A. J. Weymouth, D. Meuer, A. Liebig, A. Donarini, and F. J. Giessibl, *New J. Phys.* **24**, 083018 (2022).

- [40] A. Sweetman, S. Jarvis, R. Danza, J. Bamidele, L. Kantorovich, and P. Moriarty, *Phys. Rev. B* **84**, 085426 (2011).
- [41] R. Pawlak, W. Ouyang, A. E. Filippov, L. Kalikhman-Razvozov, S. Kawai, T. Glatzel, E. Gnecco, A. Baratoff, Q. Zheng, O. Hod, M. Urbakh, and E. Meyer, *ACS Nano* **10**, 713 (2016).
- [42] F. J. Giessibl, *Appl. Phys. Lett.* **78**, 123 (2001).
- [43] J. I. Pascual, J. Méndez, J. Gómez-Herrero, A. M. Baró, N. Garcia, U. Landman, W. D. Luedtke, E. N. Bogachek, and H. P. Cheng, *Science* **267**, 1793 (1995).
- [44] L. Kuipers and J. W. M. Frenken, *Phys. Rev. Lett.* **70**, 3907 (1993).
- [45] J. M. Krans and J. M. van Ruitenbeek, *Phys. Rev. B* **50**, 17659 (1994).
- [46] J. M. Krans, J. M. van Ruitenbeek, V. V. Fisun, I. K. Yanson, and L. J. de Jongh, *Nature (London)* **375**, 767 (1995).
- [47] H. Häkkinen, R. N. Barnett, A. G. Scherbakov, and U. Landman, *J. Phys. Chem. B* **104**, 9063 (2000).
- [48] Y. Sugimoto, A. Yurtsever, N. Hirayama, M. Abe, and S. Morita, *Nat. Commun.* **5**, 4360 (2014).
- [49] B. Enkhtaivan and A. Oshiyama, *Phys. Rev. B* **95**, 035309 (2017).
- [50] M. Ternes, C. González, C. P. Lutz, P. Hapala, F. J. Giessibl, P. Jelínek, and A. J. Heinrich, *Phys. Rev. Lett.* **106**, 016802 (2011).
- [51] N. Hauptmann, F. Mohn, L. Gross, G. Meyer, T. Frederiksen, and R. Berndt, *New J. Phys.* **14**, 073032 (2012).
- [52] Z. Ge, A. M. Graf, J. Keski-Rahkonen, S. Slizovskiy, P. Polizogopoulos, T. Taniguchi, K. Watanabe, R. Van Haren, D. Lederman, V. I. Fal'ko, E. J. Heller, and J. Velasco, *Nature (London)* **635**, 841 (2024).
- [53] Z.-G. Fu, P. Zhang, Z. Wang, and S.-S. Li, *Phys. Rev. B* **84**, 235438 (2011).
- [54] C. Zheng, Q. L. Li, B. F. Miao, L. Sun, R. Wang, X. X. Li, and H. F. Ding, *Phys. Rev. B* **96**, 235444 (2017).